Implications of Na-Ion Solvation on Na Anode-Electrolyte Interphase

S. K. Vineeth,[1,2] Chhail Bihari Soni,[1] Yongming Sun,[3] Vipin Kumar,[1,2*] Zhi Wei Seh[4*]

[1] Department of Energy Science and Engineering, Indian Institute of Technology Delhi, Hauz Khas, New Delhi, India 110016

[2] University of Queensland- IIT Delhi Academy of Research (UQIDAR), Indian Institute of Technology Delhi, Hauz Khas, New Delhi, India 110016

[3] Wuhan National Laboratory for Optoelectronics, Huazhong University of Science and Technology, Wuhan, China 430074

[4] Institute of Materials Research and Engineering, Agency for Science, Technology and Research (A*STAR), 2 Fusionopolis Way, Innovis, Singapore 138634

[*]Correspondence: vkumar@ces.iitd.ac.in (Vipin Kumar); sehzw@imre.a-star.edu.sg (Zhi Wei Seh)

Abstract

Sodium-metal anode battery technologies have revolutionized energy storage research. In recent years, new insights have been gained regarding the solid electrolyte interphase (SEI) on a sodium metal anode; however, several questions remain to be answered, in particular, the impact of electrolyte structure on the composition and physicochemical stability of the SEI. In addition, the impact of ion-solvation chemistry on the crystallinity of the SEI warrants a more detailed understanding. This review discusses the crucial aspects of sodium-ion solvation chemistry and its impact on the stability of the SEI. The core principles guiding the design of electrolytes through additives, ion-solvent interaction, and ion-pair formation are highlighted. Future research directions necessary to design a stable sodium metal anode are also discussed.

Keywords: Solid electrolyte interphase; Sodium anode; Electrolyte additives; Ionic transport; Electrode-electrolyte interface.

Na anode-electrolyte interphase

Sodium-metal batteries (SMBs) have gained significant attention in recent years owing to the high theoretical specific capacity (1166 mAh g^{-1}), high natural abundance, and low material cost of sodium [1]. However, SMBs are still plagued by numerous problems including low practical capacity, short cycle life and undesirable **dendrite formation** (see Glossary) [2]. The solid electrolyte interphase (SEI) on the sodium metal anode is considered one of the most important yet least understood components of SMBs [3]. In fact, the SEI has a direct impact on the ionic transport of sodium ions (Na^+) and hence the cycling performance of SMBs [4–6]. Precise engineering of the electrode-electrolyte interface is possible in many ways; for instance, by modifying the electrolyte constituents through additives, metal salts, and solvents [6–11]. The behavior of Na^+ transport in the SEI depends strongly on the solvation and de-solvation process, i.e., ionic migration through the interface, nature of the ion-pairs, composition, and crystalline property of the interphase [12,13]. The solvation/de-solvation process can also be influenced significantly by the magnitude of interactions between ion-ion and ion-solvent molecules [14–16], and the accumulation of ions at the electrode surface [17].

To enhance the performance of SMBs, a detailed understanding of ionic transport at the SEI is crucial. For solid crystalline materials, ionic conductivity is calculated using the Arrhenius equation [18,19]. Various diffusion models have been formulated, including direct hopping mechanism, knock-off model, and concerted migration model [20]. Direct hopping is said to occur when Na^+ diffuses to a neighboring interstitial site, while in the knock-off model, Na^+ at an interstitial site displaces different ions present at the adjacent lattice [21]. The concerted migration occurs due to complex interactions between ions, and it produces a diffusion barrier with a lower value for multiple ions than a single ion [22]. Sodium-ion/electrolyte interactions that affect ionic transport and solvation dynamics are almost similar to lithium-ion/electrolyte, despite an apparent difference in their ionic radii (ionic size of Na^+ = 1.02 Å and ionic size of Li^+ = 0.76 Å) [21,23–26]. The solvent molecules constantly interact and coordinate with metal cations due to the electronegativity difference between cations and solvent molecules [27]. They also interact with anions to modulate the dynamics of migration (through Coulombic interaction). Although the Li^+ and Na^+ ionic radii are different, there exists similar interaction with electronegative atoms of solvent molecules. However, a major difference is that Li^+ solvation structures show tetrahedral geometry, but Na^+ exists in less-ordered geometry [28]. Hence, it cannot be generalized that those electrolytes which perform well with lithium-metal batteries [28, 29] will exhibit similar characteristics for SMBs [31,32].

Successful battery operation requires optimization in selecting the right combination of battery components, including electrodes and electrolytes, thereby forming a stable SEI and enhancing battery performance [33,34]. The formation of SEI is mainly due to reduction of electrolyte molecules at the surface of metallic anode [35]. An ideal SEI allows ionic conduction while blocking electronic flow, restricting unwanted electrolyte and metal anode consumption. It also helps to screen the electrode from parasitic reactions such as polysulfide shuttle effect in metal-sulfur batteries [34]. Unstable SEI, on the other hand, leads to a non-uniform accumulation of sodium, forming sharp brush-like or mossy structures, i.e., dendrites [36], adversely affecting the Coulombic efficiency and reversible capacity. It is worth highlighting that SEI's formation characteristics directly correlate with the chemical nature of electrolytes and their additives [37,38]. Though the SEI is a complex mixture of inorganic-organic components (e.g., HCOO-Na, $ROCO_2$-Na, NaCl, NaF, Na_2CO_3, and Na_2O), it was approximated as a multi-layer arrangement by Peled and colleagues [39]. Due to heterogeneity in the chemical and physical structure of the SEI, each layer is described as a mosaic structure whose properties (i.e., composition and structure) evolve with time. Owing to the constant change in the physical and chemical composition of the SEI, the cell's performance varies with time until a stable SEI develops on the metal anode. The equivalent resistance of a mosaic SEI includes interfacial resistances, bulk resistances, and the resistances along the grain boundary [39]. Hence at the SEI, ions need to overcome numerous energy barriers as shown in Figure 1. With increase in SEI thickness, ionic conductivity decreases sharply, leading to sluggish electrochemical behavior [40]. However, engineering of electrolyte systems (through additives or co-sodium salts) can have a significant effect on the dynamics of solvation/de-solvation [41].

Understanding the physio-chemistry, composition, and nature of the SEI is of great importance while considering ionic transport and interfacial stability. Hence, this review aims to showcase the investigations to understand the factors governing solvation/de-solvation dynamics that modulate the SEI formation. Moreover, a detailed analysis of various interactions (i.e., ion-ion and other solvent molecules) that affect ion transport are summarized.

Ion-solvation chemistry of Na-ion-based electrolytes

The composition of the SEI is found to be sensitive to the ion-solvent interactions [42]. Since the lowest unoccupied molecular orbital (LUMO) contributes to electrolyte reduction, the interaction between alkali cation and solvent molecules via electrostatic interactions primarily affects the energy level of LUMO [43]. Chen and colleagues used a combination of theoretical

and experimental calculations to evaluate the reduction of electrolytes (containing Na^+ and carbonate molecules) and subsequent gas evolution at the sodium metal anode surface [44]. The calculations predicted that the gas evolution becomes severe in a Na^+-containing solvent compared to a solvent without sodium salt. Due to the formation of ion and carbonate solvent ($[NaPC]^+$ and [NaPC] complexes), the LUMO energy level lowers significantly, which is believed to facilitate gas evolution. Based on ab-initio molecular dynamics (AIMD) calculations, the solvated Na^+ preferentially breaks the C–O bond of propylene carbonate (PC) at C1–O3 and C3–O3 positions, leading to the evolution of gases, such as carbon monoxide and propane. Moreover, ion-solvent complex formation with Na^+ lowers LUMO levels for both ethylene glycol dimethyl ether (DME) and tetraethylene glycol dimethyl ether (TEGDME) as well. First principles calculations showed similar results for Li^+-solvent complexes for the other solvents, e.g., 1,3-dioxolane (DOL), see Figure 2A.

Shakourian and colleagues investigated the solvation behavior of Na^+ with various carbonate-based solvents and studied ion-solvent compatibility [45]. Based on the electronic structure of the complexes, the quantum chemistry approach was used to study ion-solvent behavior. Theoretical calculations predicted that the carbonyl oxygen is mainly accountable for facilitating interactions between Na^+ and carbonate-based solvents. Since oxygen atoms in the carbonyl groups (C=O) carry a lone pair, they preferentially interact with the solvated Na^+ ions. A decreased peak intensity of carbonyl groups indicates interaction with Na^+ ions. Due to ionic interaction between Na^+ and carbonyl groups, a shift in the highest occupied molecular orbital (HOMO) and LUMO occur towards a negative energy value. Thermochemistry calculations suggested that the interactions are favorable and exothermic, acting as the source of further interactions. Molecular dynamic (MD) simulations combined with Fourier transform infrared (FTIR) spectroscopy analysis unveiled an apparent dependency over concentration of the salt (i.e., sodium triflate (CF_3SO_3Na)) and solvation structure of diethylene glycol dimethyl ether (DEGDME) [46]. It was highlighted that ion-pairing takes place even at low concentrations (0.5 M) of CF_3SO_3Na. At a concentration of above 1.5 M, the effect of aggregation was more profound between Na^+ and triflate anion ($CF_3SO_3^-$).

The solvation of Na^+ ions can also have a direct effect on the formation of the SEI. An investigation on the comparative preferential nature of Na^+ and Li^+ ions towards carbonate solvents was conducted [47]. The interaction of ions with carbonate solvents, such as ethylene carbonate (EC), propylene carbonate (PC), dimethyl carbonate (DMC), fluoroethylene

carbonate (FEC), diethyl carbonate (DEC), and ethyl methyl carbonate (EMC), was examined. The interaction of Na^+ and Li^+ towards carbonate solvents was studied using FTIR spectroscopy, see Figure 2B-F. A weak interaction of Na^+ ions with linear carbonates was observed in FTIR spectra, which signifies a less-favorable solvation behavior of Na^+ ions with carbonate solvents. For instance, for cyclic carbonate such as PC, the interaction of Na^+ ions with carbonate chains were observed to be a little lesser than that of the interaction with Li^+ ions. The solvation of Na^+ ions with carbonate molecules was found unchanged even at higher concentrations. With the change in Na or Li salts, i.e., $NaPF_6$ or $LiPF_6$, an apparent change in the solvation behavior was noticed in IR spectra. Free energy calculations from density functional theory (DFT) showed that the combination of bi-dentate and tri-dentate are profound in the interaction between sodium salt, $NaPF_6$, and DMC. It was found that Na^+ ions exhibit weak interaction with EC compared to that of Li^+ ions, which is found to promote aggregation of sodium salt (as revealed by nuclear magnetic resonance (NMR) analysis).

Zhou and colleagues investigated the critical factors in determining the anode stability during the plating-stripping process of Na [48]. The authors introduced an anionic interfacial model for predicting the behavior and stability of Na^+-solvent at the electrode/electrolyte interface. The model considered critical factors, including binding energies of Na^+-solvent and Na^+-anion pair, anionic degree of freedom, shape, and volume of solvent and anion. The performance of the Na anode was regulated by the Na^+ solvation structure, its type, and also the location of anions, i.e., whether they are in the electrolyte bulk or close to the interface. Based on the sodium salt and solvent, the location of the anion could be predicted. The position of anion was determined using the binding energy of Na^+-anion pairs from the model, which was consistent with experimental data. The electrolyte solvation dynamics compatible with metal anode not only has a profound effect on dendrite formation, but also ensures a high Coulombic efficiency; hence consideration over solvation/de-solvation dynamics of electrolyte is an essential parameter to enhancing reversibility and stability of the metal anodes. Therefore, an optimized Na^+ solvation structure could be a novel and intriguing approach to tune the performance of high-energy rechargeable batteries.

Ion-pair formation

The interaction between ions and solvent molecules governs the solvation dynamics and other properties of the electrolyte, such as ionic conductivity and viscosity [49]. When solvent molecules surround and interact with salt ions, a diffused multi-shell network develops. This

process is called solvation (or hydration in the case of aqueous media). The solvation shell is thin in practice, which causes the electric field to become huge in close proximity of the ions (~10 MV/cm). This strong field is responsible for increasing the density of solvent molecules within the solvation shell (also called solvation number), which is highly sensitive to the physical properties, such as ionic size and dielectric permittivity of the medium. Theoretical studies conducted by Okoshi and colleagues to evaluate the solvation/de-solvation energy for Na^+ in organic solvents revealed that Na complexes exhibit much smaller solvation/de-solvation energies compared to that of Li complexes, which could be due to the weaker Lewis acidity of Na based complexes [50–52]. Additionally, the dielectric constant of the solvent (as a measure of chemical polarity) plays a vital role in determining the fundamental properties of electrolyte medium, for instance, the solvation number and tendency to form ion-pairs. Examples of ion-pairs include: (1) solvent separated ion-pairs (SSIPs) where the anion is not in the direct interaction field of the cation, (2) contact ion-pairs (CIPs) where the anion establishes an interaction with one cation only, and (3) aggregates or crystal ion-pairs (AGGs) where one anion is coordinated to two or more cations [41]. A schematic representation of the ion-pairs is shown in Figure 3A-C.

Among the carbonate solvents, EC is known to be highly polar (dielectric constant is about 89.78 at 40°C) [53]. It interacts with salt ions through dipole-dipole interactions, exhibiting a tetrahedral coordination environment of the carbonyl oxygen around Na^+, and is highly capable of dissolving large amounts of most Na electrolyte salts. Theoretical calculations have predicted that Na^+ ions are much easier to be solvated in cyclic carbonates than linear carbonates. Since EC molecules interact well with anions, this helps to form a robust protective layer on anodes, as verified in Li-ion batteries. Its high melting point (36°C) restricts it from being used as a single solvent. It hence must always be accompanied by other cyclic or linear carbonate solvents, which come at the cost of reduced thermal stability. Classical MD and DFT calculations have predicted that pure EC exhibits the highest free energy of Na^+ solvation and is preferred over PC, with an optimized mixture of EC: PC (1:1 by volume) predicted to be one of the best solvents for Na-based batteries [54]. Pham and colleagues further studied the solvation dynamics of Na^+ in EC by AIMD simulations. They identified that the solvation structure of Na^+ is highly disordered compared to Li^+ solvation with a more uniform solvation structure [55]. This leads to larger Na^+ diffusion coefficients compared to Li^+ [55,56]. While AIMD calculations shed light on the diffusion properties of Na^+, their ability to form ion pairs remains unexplored. Previous investigations have identified that the linear carbonates (e.g.,

DMC) are incompatible with Na metal anodes due to their thermodynamic restrictions [57,58]. To unveil the chemical signature of the salt, Browning and colleagues, and Patra and colleagues studied the activation energy of de-solvation and ion-pair dynamics for Na^+ in cyclic carbonates (i.e., EC and PC, and a combination thereof) [59,60]. Grand canonical Monte Carlo (GCMC) results revealed that the solvation structure of Na^+ in linear carbonates differs significantly compared to cyclic carbonates as the former favors the formation of SSIPs, which corroborated with previous findings.

Na^+ solvation is slightly more sluggish in ether-based electrolytes than carbonate solvents due to differences in solvation dynamics and lower solvent polarity [61]. Ether solvents include non-linear ethers, such as DOL and tetrahydrofuran (THF), and linear ethers of varying molecular weights ranging from DME (monoglyme), DEGDME (diglyme), to TEGDME (tetraglyme) [62]. DFT calculations performed to study Na^+ solvation dynamics in various ethers have identified that Na^+ ions can be more easily solvated in THF than the other non-linear or linear ethers [63]. As the stable thermodynamic configurations of Na^+ complexes are highly sensitive to their chemical surroundings, the solvation structure is predicted to vary for different ethers, as shown in Figure 3D,E. Despite extensive theoretical investigations, more experimental studies are nonetheless needed to verify the solvation dynamics of Na^+ complexes in ether solvents and thus pave the way for characterizing SMBs.

It is generally believed that the formation of Na dendrites or filaments formation in batteries is essentially a non-regulated Na plating process on the metal anode, wherein localized non-uniformity in current gives rise to irregular Na deposition [64–66]. Concept of deposition of sodium by engineering the host can alleviate the issue of non-uniformity in plating and striping [67]. Besides various growth models, the heterogeneous nucleation and growth model discusses the process of dendrite regulation [68]. Ely and colleagues unveiled the formation mechanism of dendrites undertaking thermodynamic as well as kinetic effects, sub-dividing the whole process into five steps: a nucleation suppression regime, a long incubation time regime, a short incubation regime, an early growth regime, and a late growth regime [69]. In the nucleation suppression regime, embryos are formed and tend to redissolve back into the electrolyte if the nucleation time is long enough for embryos to become thermodynamically stable. Thus, thermodynamically and kinetically stable nuclei formation takes place when incubation time is sufficiently short (in ms). Based on this model, a planar morphology can be achieved by regulating the flux of ions. Indeed, while dendrite growth is ubiquitous, several

strategies have been developed to regulate dendrite growth, such as guiding Na nucleation and controlling Na growth pathways and directions [70–72]. It is worth mentioning that Na dendrites are fundamentally different from their Li analogs (e.g., defect-driven dendrite growth has been established for Li, while the origin of Na dendrites is still lacking in the literature), which could be due to different chemical and mechanical properties of Na towards the reduced organic species.

In a general sense, dendrites can be considered a protruded region of an unstable metal anode; they are susceptible to external mechanical effects. Shen and colleagues evaluated the effect of pressure on dendritic growth in a coin and pouch cell [73]. Figure 4 shows the effect of external pressure on the morphology of dendrites, which affects the electrochemical performance of a Li/Cu pouch cell. Theoretical studies revealed that the optimum pressure could inhibit the growth of dendrites with smooth and branchless morphology. However, an increment in external pressure hampers the electroplating reaction and creates mechanical instabilities. Furthermore, electrolytes with lower modulus showed more pronounced suppression of dendrites.

In addition to that, dendrites can also be suppressed by creating high modular interphase, as discussed by Ferrese and colleagues [74]. Theoretical studies predicted that the separator which can withstand a pressure of 16 GPa could effectively inhibit dendrite growth through the stress created at the interfacial region of the metal anode. Despite that, the mechanical stress may negatively affect the metal anode by mechanically deforming and interfering with the thermodynamics of the anode. In addition, extended cycling causes plastic-elastic deformation at the anode, which leads to fatigue at the surface.

Effect of solvation chemistry on stability of SEI

One of the major drawbacks of conventional electrolytes is the inhomogeneity in the plating and stripping process, which leads to dendrite growth and eventual short-circuiting [75]. Several approaches have been attempted to mitigate the issues with the plating/stripping process of Na, including modification through electrolyte additives which significantly affects the deposition of Na [38,76]. Typically, electrolyte additives are the ionic salts or solvent molecules that are added in relatively smaller proportions ($1/50^{th}$ or $1/100^{th}$ compared to that of ionic salt), which has little or no effect on the bulk electrolyte. However, additives show

their effect in the interface and improve the electrochemical performance by altering the solvation and de-solvation dynamics, which eventually leads to the repair of the SEI [77].

The electrolyte additives can be classified mainly into three categories—neutral, anionic, and cationic molecules. The addition of Li^+ ions as cationic additive showed resistance to dendrite growth in Na anode, as shown in Figure 5A,B [15]. Thermodynamic analysis showed that the cation forms complex with solvent molecules and prevents electrolyte decomposition, provided the interactions between cation and solvent must be of higher magnitude than Na^+ and solvent. Moreover, additive cations ensured a smooth morphology by promoting uniform Na deposition and preventing electrolyte gassing. Solvation dynamics of Na^+ investigated using ^{23}Na-NMR spectroscopy unveiled the SEI formation process over Na anode, which is controlled mainly by the chemical structure of salt anion [41]. It was observed that for a weak-solvating solvent, e.g., DME, Lewis basicity of salt anion affects solvation of Na^+ ions. In addition to that, the attack of free radicals that are produced by chemical reduction of solvent initiates polymerization of solvent and decomposition of salt anions [41]. Sodium hexafluorophosphate ($NaPF_6$) in DME exhibited a smaller semi-circle in the Nyquist plot, indicating a lower charge-transfer resistance, which could be due to the formation of a stable and protective SEI. On the contrary, for sodium trifluoromethanesulfonate (NaOTf) and sodium perchlorate ($NaClO_4$) in DME, an increasing trend in charge-transfer resistance was observed, showing constant growth of the SEI. Besides that, severe corrosion of Na metal anode occurred in sodium trifluoromethanesulfonimide (NaTFSI) with DME. A schematic representation is shown in Figure 5C.

Bai and colleagues developed an electrolyte, which consists of 1 M $NaPF_6$ in DME with different concentrations (i.e., 0.5%, 1%, 5% and 10% by volume) of vinylene carbonate (VC) [78]. The post-deposition analysis of the SEI layer showed the presence of carbonate groups after cycling for over 2000 cycles in DME electrolyte. On the other hand, DME electrolyte with 0.5% VC showed the presence of carbonate only after 10 cycles, showing the formation of a passivation layer with the reduction of electrolyte. The chemical composition of the SEI layer and mechanical property (Young's modulus distribution) was analyzed using X-ray photoelectron spectroscopy (XPS) and atomic force microscope (AFM), respectively. O1s spectra observed at 534.2 eV suggests the reduction of VC to its polymeric form [79]. Young's modulus distribution from AFM indicates enhanced mechanical toughness due to the presence of polymeric and inorganic components present in the SEI. Besides reducing the VC molecules,

lower energy levels of the LUMO in VC-DME electrolyte promote the formation of a stable SEI during initial cycles.

Sun and colleagues reported ionic liquid electrolytes, i.e., ethylaluminum dichloride and 1-ethyl-3-methylimidazolium bis(fluorosulfonyl)imide as electrolyte additives for Na metal anode. It exhibited capacity retention of about 90% after 700 cycles [80]. The electrolyte consisted of aluminium chloride ($AlCl_3$), 1-methyl-3-ethylimidazolium chloride ([EMIm]Cl) and sodium chloride (NaCl) in addition to electrolyte additives. Delocalization of positive charges around the imidazolium ring by EMIm contributed to increasing cation-anion distance, which reduced the electrostatic interactions between ion pairs. This reduced interaction leads to enhanced ionic conduction at 25°C (9.2 mS cm^{-1}). As shown in Figure 5D-K, the SEI largely consisted of NaCl, aluminium oxide (Al_2O_3), and sodium fluoride (NaF) in addition to sodium carbonate (Na_2CO_3), sodium oxide (Na_2O), sodium sulfate (Na_2SO_4), and sodium hydroxide (NaOH), that allowed stable plating/stripping of Na. Cryo-TEM results in Figure 5H showed that the plated Na on the copper grid has a spherical morphology, diffraction patterns shown in Figure 5I,J showed the presence of Al_2O_3 and NaCl, respectively, which was consistent with elemental mapping performed using scanning transmission electron microscopy (STEM), see Figure 5K.

As SEI is a heterogeneous mixture of various organic-inorganic sodium compounds, the dissolution of SEI in electrolyte solvents is a common and challenging issue. Ma and colleagues examined electrolyte additives' critical role in inhibiting the dissolution of the SEI in liquid electrolytes [81]. They identified that with the addition of electrolyte additives (e.g., NaF and Na_2CO_3), the inorganic content of the SEI increases, which offers a longer cycle life in carbonate solvents, such as EC: DEC and PC. The electrolyte additive approach to locally repair the SEI is an innovative yet underexplored approach, and it demands much more attention to harness its full potential.

Concluding remarks

SMBs have been identified as a potential candidate for next-generation high-energy rechargeable batteries; hence, it is paramount to understand various parameters affecting their electrochemical properties. Localized interactions between Na^+ ions and electrolyte molecules are the main factors that directly correlate with the structure, composition, and physicochemical stability of the SEI. Moreover, ionic migration is dependent on the solvation/de-solvation

process, which is directly linked to the Na^+ solvation structure and the magnitude of interactions between ion-ion and ion-solvent pairs.

To improve the reversibility of sodium metal anodes, we propose a combination of multifaceted strategies, such as replacing conventional carbonates with solvents of higher LUMO energy, optimizing electrolyte additives like $SnCl_2$ and InI_3, and engineering artificial stable SEIs using 2D materials [37,38,82,83]. The compatibility of solvents and additives with the electrodes cannot be generalized, as each battery chemistry is unique. Mogensen and colleagues conducted a comprehensive investigation on a broad class of solvents and additives and their effect on the electrodes [84]. Pyrrolidone solvent, such as *N*-methyl-2-pyrrolidone, showed good cycling properties at lower current density (30 mA g^{-1}) with the lowest overall resistance. For phosphate solvent, e.g., trimethyl phosphate, the addition of sodium bis(oxalato)borate and vinylene carbonate enhanced the Coulombic efficiency above 95 %. It is apparent from the studies that the solvent performs better if mixed with other solvents compatible with each other.

Despite current developments in interfacial engineering, various challenges still need to be addressed, including understanding solvation structures and dynamics of Na^+ migration at the interface, identification, and prediction of SEI composition, and mitigation of dendritic growth (see Outstanding Questions). *Operando* characterization techniques, such as liquid-phase TEM and ambient-pressure XPS, are pivotal in addressing these issues under realistic operating conditions [85]. These strategies should be combined with state-of-the-art computations that incorporate charge and solvent effects, to provide an accurate understanding of electrified interfaces in SMBs [86]. It is anticipated that the combination of theory and experiment can be effectively applied to other promising energy storage technologies as well, such as multivalent magnesium and aluminum metal batteries [87].

Acknowledgements

Z.W.S. acknowledges the support of the Singapore National Research Foundation (NRF-NRFF2017-04). S.K.V. and C.B.S. acknowledge the scholarship awarded by the University of Queensland-IIT Delhi Academy of Research (UQIDAR) and Indian Institute of Technology Delhi (IIT Delhi).

Conflicts of interest

There are no conflicts to declare.

References

1. Matios, E. et al. (2019) Enabling Safe Sodium Metal Batteries by Solid Electrolyte Interphase Engineering: A Review. Ind Eng Chem Res. 58, 9758–9780.
2. Seh, Z. W. et al. (2015) A Highly Reversible Room-Temperature Sodium Metal Anode. ACS Cent Sci. 1, 449–455.
3. Haber, S. and Leskes, M. (2018) What Can We Learn from Solid State NMR on the Electrode-Electrolyte Interface? Adv Mater. 30, 1706496.
4. Song, J. et al. (2018) Interphases in Sodium-Ion Batteries. Adv Energy Mater. 8, 1703082.
5. Sungjemmenla et al. (2021) Unveiling the physiochemical aspects of the matrix in improving sulfur-loading for room-temperature sodium–sulfur batteries. Mater Adv. 2, 4165–4189.
6. Kumar, V. et al. (2020) A Biphasic Interphase Design Enabling High Performance in Room Temperature Sodium- Sulfur Batteries. Cell Reports Phys Sci. 1, 100044.
7. Wang, E. et al. (2021) Manipulating Electrode/Electrolyte Interphases of Sodium-Ion Batteries: Strategies and Perspectives. ACS Mater Lett. 3, 18–41.
8. Lee, J. et al. (2017) Ultraconcentrated Sodium Bis(fluorosulfonyl)imide-Based Electrolytes for High-Performance Sodium Metal Batteries. ACS Appl Mater Interfaces. 9, 3723–3732.
9. Sun, B. et al. (2020) Design Strategies to Enable the Efficient Use of Sodium Metal Anodes in High-Energy Batteries. Adv Mater. 32, 1903891.
10. Kumar, V. et al. (2020) An artificial metal-alloy interphase for high-rate and long-life sodium–sulfur batteries. Energy Storage Mater. 29, 1–8.
11. Jishnu, N. S. et al. (2021) Electrospun PVdF and PVdF-co-HFP-Based Blend Polymer Electrolytes for Lithium Ion Batteries; *Electrospinning for Advanced Energy Storage Applications*; Balakrishnan, N. T. M, Prasanth, R.; pp. 201–234, Singapore: Springer Singapore.
12. Monti, D. et al. (2020) Towards standard electrolytes for sodium-ion batteries: physical properties, ion solvation and ion-pairing in alkyl carbonate solvents. Phys Chem Chem Phys. 22, 22768–22777.
13. Siegel, D. J. et al. (2021) Establishing a unified framework for ion solvation and transport in liquid and solid electrolytes, Trends Chem. 3, 807-818.

14. Kulkarni, P. et al. (2021) Recent progress in ‘water-in-salt’ and ‘water-in-salt’-hybrid-electrolyte-based high voltage rechargeable batteries. Sustain Energy Fuels. 5, 1619–1654.
15. Chen, X. et al. (2020) Ion-Solvent Chemistry-Inspired Cation-Additive Strategy to Stabilize Electrolytes for Sodium-Metal Batteries. Chem. 6, 2242–2256.
16. Li, Y. et al. (2019) Intercalation chemistry of graphite: alkali metal ions and beyond. Chem Soc Rev. 48, 4655–4687.
17. Raguette, L. and Jorn, R. (2018) Ion Solvation and Dynamics at Solid Electrolyte Interphases: A Long Way from Bulk? J Phys Chem C. 122, 3219–3232.
18. Petrowsky, M. and Frech, R. (2010) Application of the Compensated Arrhenius Formalism to Self-Diffusion: Implications for Ionic Conductivity and Dielectric Relaxation. J Phys Chem B. 114, 8600–8605.
19. Nuernberg, R. B. (2020) Numerical comparison of usual Arrhenius-type equations for modeling ionic transport in solids. Ionics (Kiel). 26, 2405–2412.
20. Lee, B. et al. (2019) Sodium Metal Anodes: Emerging Solutions to Dendrite Growth. Chem Rev. 119, 5416–5460.
21. Yildirim, H. et al. (2015) First-Principles Analysis of Defect Thermodynamics and Ion Transport in Inorganic SEI Compounds: LiF and NaF. ACS Appl Mater Interfaces. 7, 18985–18996.
22. He, X. et al. (2017) Origin of fast ion diffusion in super-ionic conductors. Nat Commun. 8, 15893.
23. Shi, S. et al. (2012) Direct Calculation of Li-Ion Transport in the Solid Electrolyte Interphase. J Am Chem Soc. 134, 15476–15487.
24. Xu, Y. et al. (2013) Electrochemical Performance of Porous Carbon/Tin Composite Anodes for Sodium-Ion and Lithium-Ion Batteries. Adv Energy Mater. 3, 128–133.
25. Mei, J. et al. (2019) Cobalt oxide-based nanoarchitectures for electrochemical energy applications. Prog Mater Sci. 103, 596–677.
26. Zheng, X. et al. (2021) Tailoring Electrolyte Solvation Chemistry toward an Inorganic-Rich Solid-Electrolyte Interphase at a Li Metal Anode. ACS Energy Lett. 6, 2054–2063.
27. Morales, D. et al. (2021) Transport studies of NaPF6 carbonate solvents-based sodium ion electrolytes. Electrochim Acta. 377, 138062.
28. Nayak, P. K. et al. (2018) From Lithium-Ion to Sodium-Ion Batteries: Advantages, Challenges, and Surprises. Angew Chem Int Ed Engl. 57, 102–120.

29. Lu, D. et al. (2015) Failure Mechanism for Fast-Charged Lithium Metal Batteries with Liquid Electrolytes. Adv Energy Mater. 5, 1400993.
30. Yu, L. et al. (2018) A Localized High-Concentration Electrolyte with Optimized Solvents and Lithium Difluoro(oxalate)borate Additive for Stable Lithium Metal Batteries. ACS Energy Lett. 3, 2059–2067.
31. Xu, C. et al. (2020) Electrolytes for Lithium- and Sodium-Metal Batteries. Chem – An Asian J. 15, 3584–3598.
32. Hwang, J-Y. et al. (2017) Sodium-ion batteries: present and future. Chem Soc Rev. 46, 3529–3614.
33. Li, T. et al. (2019) The latest advances in the critical factors (positive electrode, electrolytes, separators) for sodium-sulfur battery. J Alloys Compd. 792, 797–817.
34. Eng A. Y. S. et al. (2021) Room-Temperature Sodium–Sulfur Batteries and Beyond: Realizing Practical High Energy Systems through Anode, Cathode, and Electrolyte Engineering. Adv Energy Mater. 11, 2003493.
35. Chawla, N. and Safa, M. (2019) Sodium Batteries: A Review on Sodium-Sulfur and Sodium-Air Batteries. Electronics. 8, 1201.
36. Wei, S. et al. (2017) Highly Stable Sodium Batteries Enabled by Functional Ionic Polymer Membranes. Adv Mater. 29, 1605512.
37. Xu, X. et al. (2018) A room-temperature sodium–sulfur battery with high capacity and stable cycling performance. Nat Commun. 9, 3870.
38. Zheng, X. et al. (2019) Toward a Stable Sodium Metal Anode in Carbonate Electrolyte: A Compact, Inorganic Alloy Interface. J Phys Chem Lett. 10, 707–714.
39. Peled. E. et al. (1997) Advanced Model for Solid Electrolyte Interphase Electrodes in Liquid and Polymer Electrolytes. J. Electrochem. Soc. 144, L208-L210.
40. Lee, J. et al. (2020) A review on recent approaches for designing the SEI layer on sodium metal anodes. Mater Adv. 1, 3143–3166.
41. Lutz, L. et al. (2017) Role of Electrolyte Anions in the Na–O 2 Battery: Implications for NaO 2 Solvation and the Stability of the Sodium Solid Electrolyte Interphase in Glyme Ethers. Chem Mater. 29, 6066–6075.
42. Bao, C. et al. (2020) Solid Electrolyte Interphases on Sodium Metal Anodes. Adv Funct Mater. 30, 2004891.
43. Chen, X. et al. (2021) Ion–solvent chemistry in lithium battery electrolytes: From mono-solvent to multi-solvent complexes. Fundam Res. 1, 393–398.

44. Chen, X. et al. (2018) Ion–Solvent Complexes Promote Gas Evolution from Electrolytes on a Sodium Metal Anode. Angew Chemie Int Ed. 57, 734–737.
45. Shakourian-Fard, M. et al. (2015) Trends in Na-Ion Solvation with Alkyl-Carbonate Electrolytes for Sodium-Ion Batteries: Insights from First-Principles Calculations. J Phys Chem C. 119, 22747–22759.
46. Wahlers, J. et al. (2016) Solvation Structure and Concentration in Glyme-Based Sodium Electrolytes: A Combined Spectroscopic and Computational Study. J Phys Chem C. 120, 17949–17959.
47. Cresce, A. V. et al. (2017) Solvation behavior of carbonate-based electrolytes in sodium ion batteries. Phys Chem Chem Phys. 19, 574–586.
48. Zhou, L. et al. (2020) Engineering Sodium-Ion Solvation Structure to Stabilize Sodium Anodes: Universal Strategy for Fast-Charging and Safer Sodium-Ion Batteries. Nano Lett. 20, 3247–3254.
49. Andreev, M. et al. (2018) Influence of Ion Solvation on the Properties of Electrolyte Solutions. J Phys Chem B. 122, 4029–4034.
50. Okoshi, M. et al. (2018) Theoretical Analysis of Carrier Ion Diffusion in Superconcentrated Electrolyte Solutions for Sodium-Ion Batteries. J Phys Chem B. 122, 2600–2609.
51. Okoshi, M. et al. (2013) Theoretical Analysis on De-Solvation of Lithium, Sodium, and Magnesium Cations to Organic Electrolyte Solvents. J Electrochem Soc. 160, A2160–A2165.
52. Okoshi, M. et al. (2017) Theoretical Analysis of Interactions between Potassium Ions and Organic Electrolyte Solvents: A Comparison with Lithium, Sodium, and Magnesium Ions. J Electrochem Soc. 164, A54–A60.
53. Ding, M. S. et al. (2000) Liquid-Solid Phase Diagrams of Binary Carbonates for Lithium Batteries. J Electrochem Soc. 147, 1688.
54. Tiwari, S. et al. (2021) Studies on the interaction of Na + ion with binary mixture of carbonate-ester solvents: A density functional theory approach. J Phys Conf Ser. 1849, 012024.
55. Pham, T. A. et al. (2017) Solvation and Dynamics of Sodium and Potassium in Ethylene Carbonate from ab Initio Molecular Dynamics Simulations. J Phys Chem C. 121, 21913–21920.
56. Pham, T. A. (2019) Ab initio simulations of liquid electrolytes for energy conversion and storage. Int J Quantum Chem. 119, 1–13.

57. Eshetu, G. G. et al. (2020) Electrolytes and Interphases in Sodium-Based Rechargeable Batteries: Recent Advances and Perspectives. Adv Energy Mater. 10, 2000093.
58. Yan, G. et al. (2018) Assessment of the Electrochemical Stability of Carbonate-Based Electrolytes in Na-Ion Batteries. J Electrochem Soc. 165, A1222–A1230.
59. Patra, J. et al. (2019) Moderately concentrated electrolyte improves solid–electrolyte interphase and sodium storage performance of hard carbon. Energy Storage Mater. 16, 146–154.
60. Browning, K. L. et al. (2017) Energetics of Na + Transport through the Electrode/Cathode Interface in Single Solvent Electrolytes. J Electrochem Soc. 164, A580–A586.
61. Karatrantos, A. et al. (2018) The effect of different organic solvents on sodium ion storage in carbon nanopores. Phys Chem Chem Phys. 20, 6307–6315.
62. Lin, Z. et al. (2019) Recent research progresses in ether- and ester-based electrolytes for sodium-ion batteries. InfoMat. 1, 376–389.
63. Liu, Q. et al. (2020) A theoretical study on Na + solvation in carbonate ester and ether solvents for sodium-ion batteries. Phys Chem Chem Phys. 22, 2164–2175.
64. Delmas, C. (2018) Sodium and Sodium-Ion Batteries: 50 Years of Research. Adv Energy Mater. 8, 1703137.
65. Zhao, Y. et al. (2018) Recent developments and insights into the understanding of Na metal anodes for Na-metal batteries. Energy Environ Sci. 11, 2673–2695.
66. Wang, Y-X. et al. (2017) Room-Temperature Sodium-Sulfur Batteries: A Comprehensive Review on Research Progress and Cell Chemistry. Adv Energy Mater. 7, 1602829.
67. Soni, C. B. et al. (2021) Guiding Uniform Sodium Deposition through Host Modification for Sodium Metal Batteries. Batter. Supercaps. https://doi.org/10.1002/batt.202100207.
68. Barai, P. et al. (2017) Lithium dendrite growth mechanisms in polymer electrolytes and prevention strategies. Phys Chem Chem Phys. 19, 20493–20505.
69. Ely, D. R. et al. (2014) Phase field kinetics of lithium electrodeposits. J Power Sources. 272, 581–594.
70. Soni, C. B. et al. (2021) Challenges in regulating interfacial-chemistry of the sodium-metal anode for room-temperature sodium-sulfur batteries. Energy Storage. e264. https://doi.org/10.1002/est2.264.

71. Yan, K. et al. (2020) Dendrite-Free Sodium Metal Batteries Enabled by the Release of Contact Strain on Flexible and Sodiophilic Matrix. Nano Lett. 20, 6112–6119.
72. Xu, Y. et al. (2020) Sodium Deposition with a Controlled Location and Orientation for Dendrite-Free Sodium Metal Batteries. Adv Energy Mater. 10, 2002308.
73. Shen, X. et al. (2021) How Does External Pressure Shape Li Dendrites in Li Metal Batteries?, Adv. Energy Mater. 11, 2003416.
74. Ferrese, A. and Newman, J. (2014) Mechanical Deformation of a Lithium-Metal Anode Due to a Very Stiff Separator, J. Electrochem. Soc. 161, A1350–A1359.
75. Ma, L. et al. (2020) Dendrite-free lithium metal and sodium metal batteries. Energy Storage Mater. 27, 522–554.
76. Chen, Q. et al. (2020) Building an artificial solid electrolyte interphase with high-uniformity and fast ion diffusion for ultralong-life sodium metal anodes. J Mater Chem A. 8, 16232–16237.
77. Fan, L. and Li, X. (2018) Recent advances in effective protection of sodium metal anode. Nano Energy 53, 630–642.
78. Bai, P. et al. (2020) Solid electrolyte interphase manipulation towards highly stable hard carbon anodes for sodium ion batteries. Energy Storage Mater. 25, 324–333.
79. Michan, A. L. et al. (2016) Fluoroethylene Carbonate and Vinylene Carbonate Reduction: Understanding Lithium-Ion Battery Electrolyte Additives and Solid Electrolyte Interphase Formation. Chem Mater. 28, 8149–8159.
80. Sun, H. et al. (2019) A safe and non-flammable sodium metal battery based on an ionic liquid electrolyte. Nat Commun. 10, 3302.
81. Ma, L. A. et al. (2021) Strategies for Mitigating Dissolution of Solid Electrolyte Interphases in Sodium-Ion Batteries, Angew. Chemie - Int. Ed. 60, 4855–4863
82. Eng, A. Y. S. et al. (2020) Tailoring binder–cathode interactions for long-life room-temperature sodium–sulfur batteries. J Mater Chem A. 8, 22983–22997.
83. Tian, H. et al. (2017) Theoretical Investigation of 2D Layered Materials as Protective Films for Lithium and Sodium Metal Anodes. Adv Energy Mater. 7, 1602528.
84. Mogensen, R. et al. (2021) An Attempt to Formulate Non-Carbonate Electrolytes for Sodium-Ion Batteries, Batteries Supercaps. 4, 791–814.
85. Handoko, A. D. et al. (2018) Understanding heterogeneous electrocatalytic carbon dioxide reduction through operando techniques. Nat Catal. 1, 922–934.
86. Steinmann, SN. and Seh, Z. W. (2021) Understanding electrified interfaces. Nat Rev Mater. 6, 289–291.

87. Nguyen, D-T. et al. (2021) Material design strategies to improve the performance of rechargeable magnesium–sulfur batteries. Mater Horizons. 8, 830–853.

Figures.

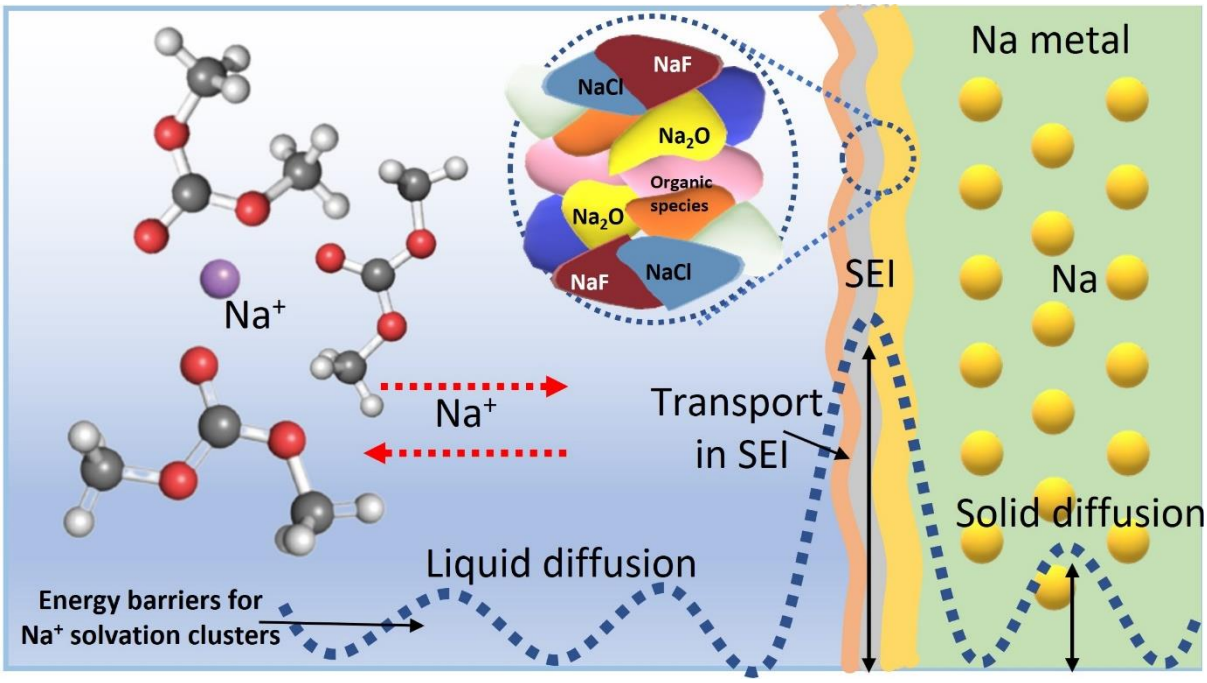

Figure 1. Schematic representation of Na^+ transport at the interface of electrolyte/sodium metal anode. SEI is depicted as a complex mixture of sodium compounds due to the reduction of electrolyte molecules at the surface of the sodium metal anode.

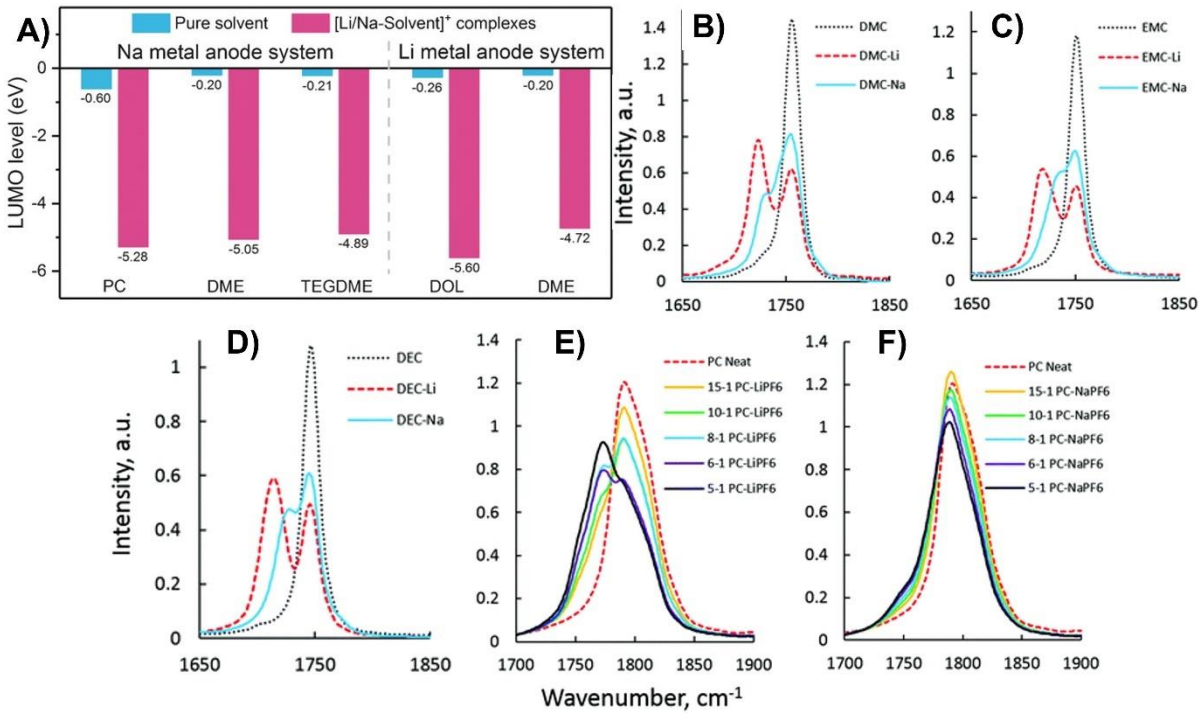

Figure 2. Ion-solvation chemistry in electrolytes. A) Comparative value of LUMO levels for pure solvent and complex formed using Na^+ and Li^+. Reproduced, with permission, from [44]. B-F) Overlaid FTIR spectra showing a comparison of interaction between Na^+ and Li^+ towards carbonate solvents namely B) DMC, C) EMC, (D) DEC, (E, F) PC- Li^+ and PC- Na^+ at various mole ratios. Reproduced, with permission, from [47].

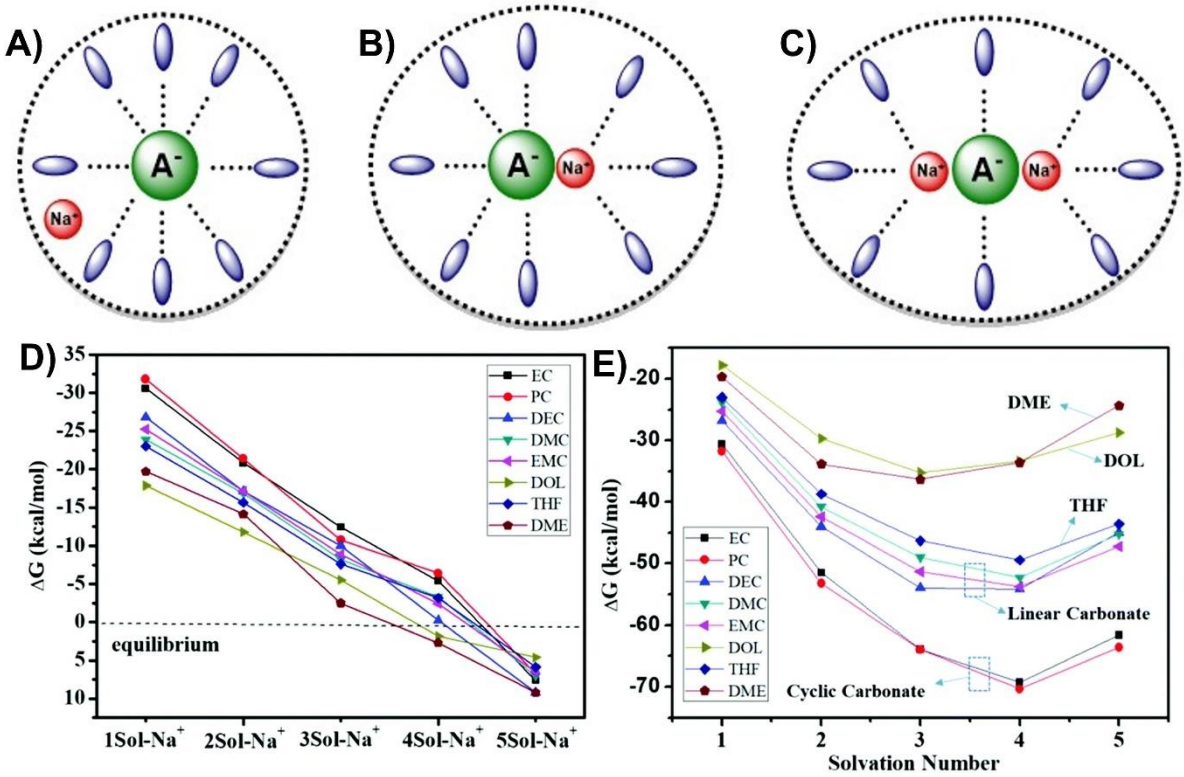

Figure 3. Ion-pair formation in electrolytes. A-C) Schematic representation of various ion-pair formations between sodium cation and solvent anion, namely, A) Solvent separated ion-pair (SSIP), B) contact ion-pair (CIP), and C) aggregates or crystal ion-pair (AGG). D) Stepwise Na^+ solvation reaction Gibbs free energy curves in different solvents with the change in solvent numbers, E) The overall Na^+ solvation reaction Gibbs free energy curves in different solvation numbers. Reproduced, with permission, from [63].

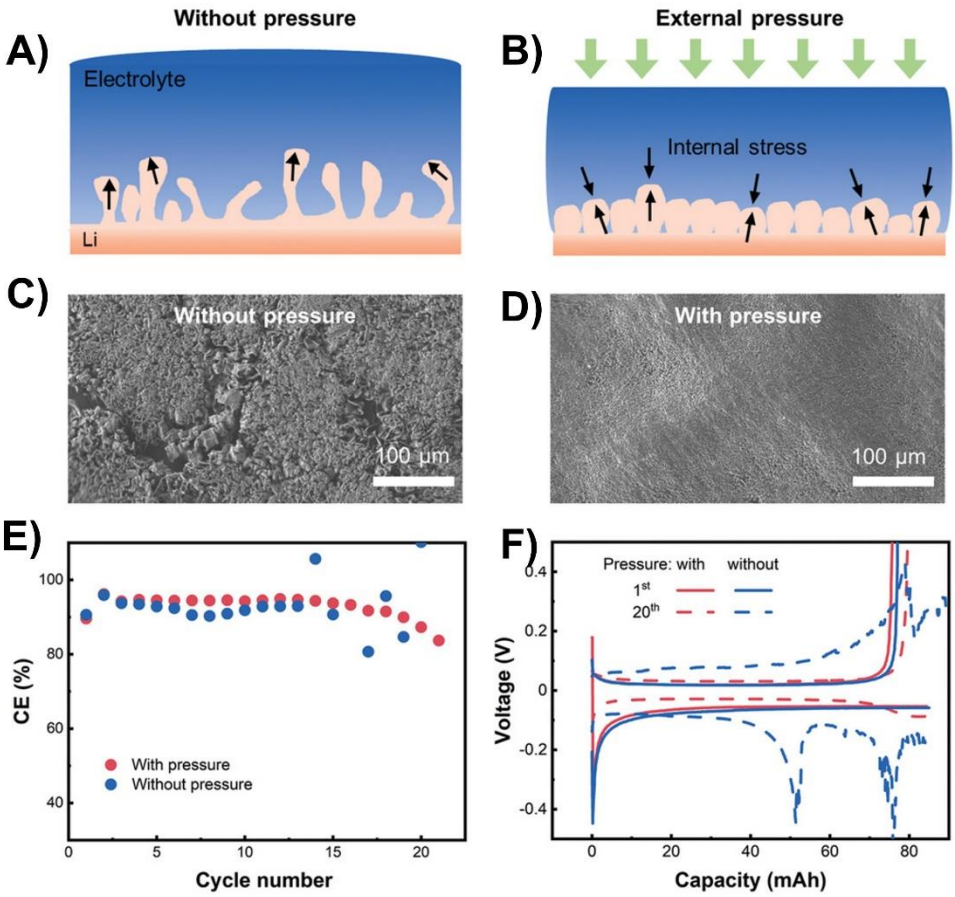

Figure 4. Comparison of the effect of pressure on dendrite growth over lithium metal anode. A, B) Representation of dendritic growth at anode-electrolyte interface without external pressure and upon application of external pressure. C, D) SEM morphology of electroplated lithium without and with external pressure. E) Variation in Coulombic efficiency at various cycles with and without the application of external pressure, measured using Li|Cu pouch cell. F) Respective polarization curves measured at 1 mA cm^{-2} current density and 3 mAh cm^{-2} capacity. Reproduced, with permission, from [73].

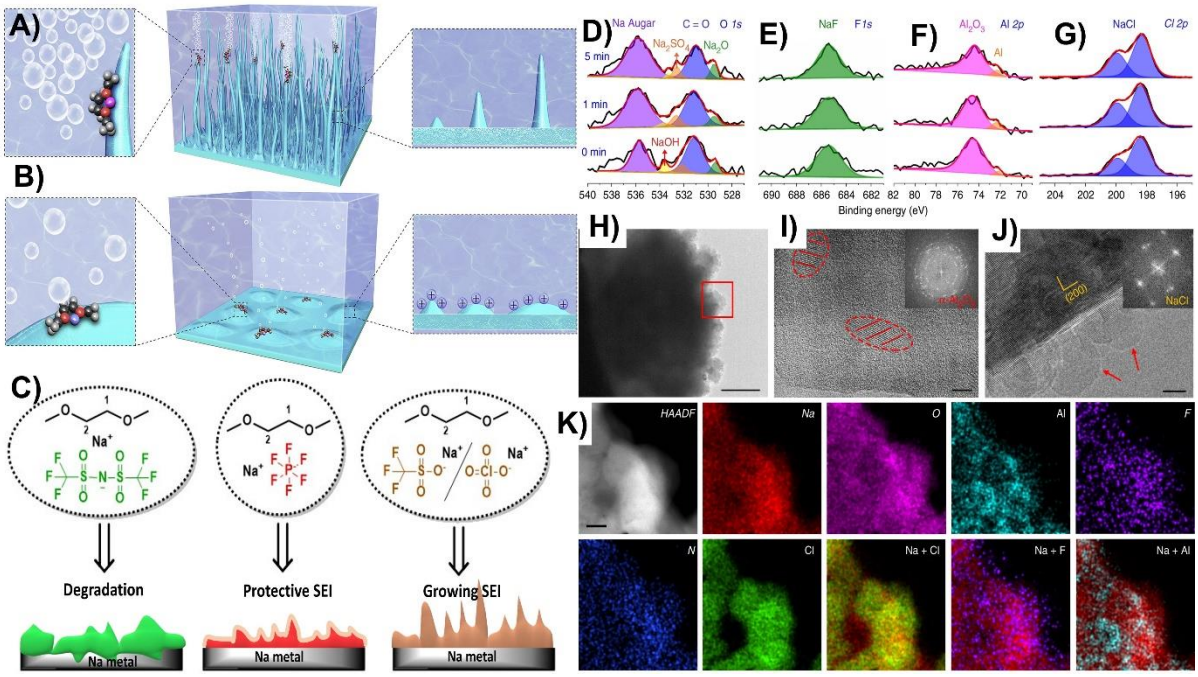

Figure 5. Schematic representation on the effect of addition of cationic additive on the anode. A) Pristine electrolyte, leading to dendrite growth and gassing phenomenon, and B) electrolyte containing cationic additive, showing prohibition of gassing and dendrite growth. Reproduced, with permission, from [15]. C) Influence of various sodium salts in DME on SEI layer. D-G) XPS spectra (high resolution) of SEI layer. H) Cryo-TEM of sodium plated on copper grid at a current density of 0.1 mA cm^{-2}, with 500 nm scale bar. I, J) High-resolution Cryo-TEM images and diffraction patterns (inset) of SEI for Al_2O_3 and NaCl, with 5 nm scale bar. K) High-angle annular dark-field (HAADF) and the respective element mapping images, taken by scanning transmission electron microscopy (STEM), with 100 nm scale bar. Reproduced, with permission, from [80].